Journal of Applied Fluid Mechanics, Vol. 10, No. 4, pp. 1079-1089, 2017.
Available online at www.jafmonline.net, ISSN 1735-3572, EISSN 1735-3645.
DOI: 10.18869/acadpub.jafm.73.241.27589

Experimental and Theoretical Investigation on the Effect of Pumped Water Temperature on Cavitation Breakdown in Centrifugal Pumps

M. A. Hosien† and S. M. Selim

Mechanical Power Engineering Department, Faculty of Engineering, Menoufyia University, Shebin El-Kom, Egypt

†*Corresponding Author Email: mohamed_abdelaziz14@yahoo.com*

(Received January 12, 2017; accepted March 15, 2017)

ABSTRACT

Cavitation breakdown at various liquid temperatures is one of the major problems encountered in the operations of centrifugal pumps. There are a number of practical cases where the pumps operate at high temperature or near the saturation temperature of the liquid. A detailed understanding of the factors affecting the breakdown of cavitation is essential for accurate performance prediction and design. The purpose of this paper is to present results of a cavitation breakdown investigation which are both experimental and theoretical. The present model based on Rayleigh-Plesset expression for bubble dynamics. The predicted model includes many important parameters controlling the cavitation breakdown such as bubble dynamics, flow rate, rotational speed, temperature and thermodynamics properties of water and the gas pressure inside the cavity. The present model has been tested against extensive present and earlier published experimental results in centrifugal pumps at various operating water temperatures and operating conditions. The comparison between the predicted breakdown blade cavitation number with the present and previous published experimental results showed a surprisingly good agreement. This agreement means that the roles played by many important parameters are consistent with the present model. Therefore, the present model represents an addition to knowledge in this aspect which could help the centrifugal pump user and designer to predict the breakdown cavitation performance at various operating conditions.

Key words: Cavitation; Breakdown; Thermodynamic effect; Centrifugal pump.

NOMENCLATURE

C_{m1}	meridional velocity at the inlet of the blade
h_{fg}	latent heat of vaporization
Ns	pump specific speed
NPSH	Net Positive Head
p_{atm}	atmospheric pressure
p_G	pressure of the gas within the bubble
p_{suc}	pump suction pressure
p_v	vapour pressure
Q_n	nominal pump flow rate
$\dot{Q}$	volumetric flow rate
R	radius of the bubble
R_0	initial radius of the bubble nuclei
S	surface tension
t	time
T	temperature
U	peripheral speed or flow velocity
γ	specific weight of liquid
σ_b	blade cavitation number
σ_B	breakdown cavitation number
ρ_V	vapour density
ρ_L	liquid density
μ	absolute viscosity

1. INTRODUCTION

Cavitation produces deleterious effects for hydraulic machinery, hydrofoils, dams, cylinder liners, valves and sluice gates. In pumps these effects generally result in loss in head and efficiency and increase in power consumption. Cavitation also causes vibration, noise, alteration of flow pattern. For these reasons, speeds and suction pressure are limited to avoid these effects for hydraulic machinery, although, for commercial reasons, a limited amount of cavitation is often allowed and the resulting risk of erosion damage accepted, Pearsall (1973). There are a number of

cases where, these limitations are acceptable. Such cases are rockets, and aircraft pumps, where high speed pumps are required for low-weight reasons. In addition, boiler feed pump operates near the saturation temperature of the water. Using a cavitating pump enables speeds to be raised and this has economic as well as mechanical advantages as a reduction in the size and the number of stages is possible. Also erosion damage may be avoided (Gongwer, 1941; Pearsall, 1972 and Pearsall, 1973). Therefore, a fuller basic understanding of pump performance when cavitation takes place has become important in the design of higher specific speed machinery. This interest stems from the need to minimize the weight of space launch vehicles in order to increase the payload capability of the rocket. So, reliable information about cavitation breakdown of pumps at various operating conditions is necessary.

Hofmann *et al.* (2001) presented experimental and numerical study concerning the pump characteristics and performance breakdown. The results were drawn and compared at different flow conditions and the mean spatial distributions of vapour structures within the runner. Besides the measurements of the characteristics of the pump at different flow rates and cavitation conditions, various visualization techniques were used. All images shown in the mentioned paper were done at nominal flow rate with various values of NPSH, where both cavitations on suction and pressure side of the blades occurs.

Visser (2005) predicted incipient cavitation ($NPSH_i$) and $NPSH_{3\%}$ calculated head drop curves from CFD cavitation models.

Li *et al.* (2006) developed cavitation model and algorithm for predicting hydrodynamic performance of a centrifugal pump under cavitating condition. The capability to capture some important phenomena of cavitation flows in a centrifugal pump impeller was shown by the cavitation prediction. The numerical results also showed that the cavity size increases dramatically with the decrease in the cavitation number and so does the loss of the head rise.

Cavitation performance depends on temperature of liquid and type of liquid.

Pierrat *et al.* (2008) presented a study of the leading edge cavitation. The impeller of a single stage helico-centrifugal pump, a specific impeller with transparent shroud and a special casing with windows have been used as experimental test rig. The leading edge cavitation has been experimentally observed on the both sides of the impeller and the head drop measured for different operating conditions. A CFD model for cavitation simulation has been investigated and compared to experimental results for the three values of flow rates, ranging from 0.85 Q_n to 1.25 Q_n. The model used a multiphase approach, based on a homogeneous model assumption. A truncated form of Rayleigh-Plesset equation is used as a source term for the inter-phase mass transfer. The cavitation figures are in a good agreement with the experimental ones for each flow rate.

Liu *et al*. (2013) presented a modified k-ω model and introduced a cavitation model frequently used in hydrofoils and propellers to model the cavitating flow in a centrifugal pump. The numerical investigation clearly demonstrates that the breakdown of pump performances is mainly due to the development of cavitation. The vapor-filled cavities attaching on blades fill up the impeller passage, resulting in the flow separating from the blades, and consequently the drop of the head coefficient.

Li (2014) applied full cavitation model in the cavitating flow simulation and the cavitation performance prediction of a centrifugal pump to improve or optimize its hydraulic design. Since the model involves surface tension and non-condensable gas content, it can be potentially applied in predicting cavitation behavior of a centrifugal pump when handling viscous oils that possess different surface tension and gas content than water.

(2015) conducted experimental and numerical research to investigate the influence of prewhirl regulation by inlet guide vanes on cavitation performance and flow characteristic in a centrifugal pump.

Jain *et al.* (2016) applied cavitation model based on Rayleigh-Plesset equation to simulate 3-D turbulent flow field and to predict cavitation performance of multistage centrifugal pump. The comparison of calculated value and measured result showed that the cavitation model was more reasonable at designed condition and low flow rate condition.

Mostafa *et al.* (2016) simulate cavity over a hydrofoil under different cavitation numbers and angle of attacks using bubble dynamics cavitation.

Because of this situation, the present investigation is intended to find precisely the effects of water temperature, pump flow rate, and rotational speed on cavitation breakdown performance of centrifugal pump.

2. EXPERIMENTAL WORK

2.1 Experimental Apparatus and Instrumentation

In the present study experiments were conducted to investigate the effect of flow rate ratio, water temperature and the pump rotational speed on the breakdown cavitation number. A study of the effect of flow rate ratio on the breakdown cavitation number was conducted over a wide range of water temperatures, rotational speeds and flow rates. The experimental data were obtained by conducting experiments using a specially designed and fabricated experimental facility. Details of the test rig are shown in Selim *et al.* (2009).

Briefly, the flow system consists of 7.5 HP single stage centrifugal pump, working inlet transparent perspex section, the main tank, the flow meter, orifice, measuring devices, pipelines, and valves. The pump inlet section and the impeller front shroud were made of transparent perspex to permit visual

study. The type of the plain impeller of the pump is a closed impeller with six curved vanes. The inside and outside diameters of the impeller are 5.4 cm and 17.5 cm. The inlet and outlet blade angles are 21.5˚ and 28˚. The blade heights at inlet and outlet are 10.5 mm and 5 mm, respectively. The driving electric motor is 7.5 HP A.C. motor, running at a nominal speed of 2920 rpm connected to the pump by rigid coupling. The specific speed of the pump Ns = 0.321.

The pump performance characteristics were performed at different water temperatures varying from 20˚C to 90˚C. A mercury thermometer is used to measure the water temperature at the pump inlet and the delivery line. The accuracy of the thermometer is ± 1% from measured quantity of the temperature. The measuring span is 0-120˚C. Experiments were conducted at rotation speeds of 2600, 2800 and 3000 rpm. The flow rate through the pump was measured by using a calibrated orifice in addition to an electromagnetic flow meter. The accuracy of measuring the flow rate using the calibrated orifice by measuring the difference in head of mercury manometer was ± 0.028% from the measured quantity of the flow rate. While, the accuracy of measuring flow rate using electromagnetic flow meter was ± 1% from measured value of the flow rate. The flow rate tested was ranged from 1.86×10^{-3} to 7.645×10^{-3} m^3/s.

The manometric delivery head was measured by using calibrated Bourdon pressure gauge in the range of 0 – 6 bar. The accuracy of the gauge was ± 0.49% of span. The manometric suction head was measured by using calibrated Bourdon vacuum pressure gauge in the range of 0 – (-1) bar, with an accuracy of $\pm$ 1.2% of span.

The atmospheric pressure was measured by using mercury barometer with an accuracy of $\pm$ 0.0262% of span.

Visual observation of cavitation inception was achieved by a transparent perspex cover with a digital stroboscopic light. The model of stroboscope is DS-303, 240 Volt, 100 Watts, and the frequency ranged from 50 Hz to 60 Hz.

The rotation speed in revolution per minute was measured by using an inverter type model: L100 - 055HFE. HP/kW: 7.5/5.5. The L100 delivers speed regulation (no load to full load) within 3% of the (full scale) motor nameplate speed value. A speed inverter of type Hitachi L100 has been used to provide control for 3-phase AC induction motors.

The suction static lift of 0.67 m was kept constant, and it was checked repeatedly during the tests. The experiments were carried out at almost equal room temperature of 25 ^oC ± 1 ^oC and atmospheric pressure in order to obtain more accurate results. The experimental readings were taken carefully, tabulated and then plotted graphically.

2.2. Testing Procedures

The performance of the pump with cavitation condition was conducted at constant speed and constant flow rate. In this method, the flow rate was set to arbitrary values in the range of 1.86×10^{-3} to 7.645×10^{-3} m^3/s. Then the suction pressure was decreased step by step at a constant value of flow rate, until the visual breakdown cavitation condition occurred. The breakdown means the cavity is indefinitely long. The measurements of pressures, temperature and speed corresponding to the breakdown condition were noted.

The Net Positive Suction Head (NPSH) is given by the following expression:

$$\mathrm{NPSH} = \frac{p_{atm}}{\gamma} \pm \frac{p_{suc}}{\gamma} - \frac{p_v}{\gamma} \tag{1}$$

The blade cavitation number (σ_b) is given by:

$$\sigma_b = \frac{p_1 - p_v}{\frac{1}{2}\rho U_1^2} \tag{2}$$

Equations (1) and (2), the relation between the NPSH and σ_b is:

$$\mathrm{NPSH} = \frac{C_{m1}^2}{2g}(\sigma_b + 1 + \lambda) + \sigma_b \frac{U_1^2}{2g} \tag{3}$$

σ_b : is the blade cavitation number.

λ : is the contraction loss constant ($\lambda = 0.045$) , C_{m1} is the meridional velocity at the inlet of the blade, U_1 is the peripheral velocity at the inlet of the impeller, p_1 is static pressure at the front of the blade, p_{atm} is the atmospheric pressure and p_v is the vapour pressure. The maximum and minimum uncertainties in the blade cavitation number are 3.76% and 0.992%, respectively and in the head ratio are 0.85% and 0.3%, respectively.

3. THEORETICAL CONSIDERATIONS

The effects of liquid properties and liquid temperatures on cavitation characteristics of pumps have been studied for many years and much work has been done in trying to predict the performance of pumps from tests made with cold water.

It has been experimentally established that the cavitation characteristics of pumps supplying liquid at high temperatures are different from the corresponding characteristics obtained with cold water. The previous work suggests that the observed change in the pump cavitation performance when supplying liquids at high temperature results from a difference between vapour pressure corresponding to free stream temperature and the cavity pressure, the magnitude of this difference increases with increasing temperature. Thus, the apparent increase in cavitation performance that is noted at higher temperatures (i.e. the reduction in break–off NPSH) can be attributed to evaporative cooling of the liquid during the vaporization process and this cooling is a function of fluid properties and temperature (thermodynamic effects). This effect will occur in any liquid and becomes more significant as the temperature is increased.

The thermodynamic effect is dependent upon the energy requirement for the vaporization process which occurs at the cavity wall. As a result of this energy requirement, the temperature in the cavity is less than that of the bulk fluid, and this causes a correspondingly reduced cavity pressure. The

determination of cavity pressure thus becomes of primary importance in cavitating flows.

In many cases the cavity pressure is assumed to be equal to the vapour pressure at bulk fluid temperature. This estimate is reasonable in the absence of non-condensable gases where the vapour pressure p_v and the gradient of the vapour pressure (dp_v/dT) in respect to temperature are both small, which occurs at states significantly below the critical temperature. However, for some liquids, the operating temperatures can be such that p_v and (dp_v/dT) are both large. In these cases the assumption that the cavity pressure is equal to the liquid vapour pressure can lead to very large errors in predicting performance.

Most of the progresses in understanding the details of the cavitation processes have been made through the consideration of the dynamic equilibrium of a spherical bubble containing vapour and non-condensable gas. The equation of motion of cavitation bubbles produced by the pressure field around a body in an incoming liquid, first formulated by Rayleigh was modified by Plesset and Prosperetti (1977). The Rayleigh-Plesset equation is given by:

$$\rho_L\left(R\ddot{R}+\frac{3}{2}\dot{R}^2\right)=p_G-2S/R-4\mu\dot{R}/R+\left[C_p(t)-\sigma_l-C_T(t)\right]\frac{1}{2}\rho_L U_\infty^2 \quad (4)$$

where

$$\sigma_l = (p_\infty - p_v(T_\infty))/(\tfrac{1}{2}\rho_L U_\infty^2) \quad (5)$$

$$C_P(t) = (p_\infty - p_L(t))/(\tfrac{1}{2}\rho_L U_\infty^2) \quad (6)$$

$$C_T(t) = (p_v(T_\infty) - p_v(T_R))/(\tfrac{1}{2}\rho_L U_\infty^2) \quad (7)$$

where

$$\dot{R} = \frac{dR}{dt}\ ,\ \ddot{R} = \frac{d^2R}{dt^2}$$

The problem to be solved is that of a spherical bubble of initial radius R_0 containing both non-condensable (and no diffusing) gas and saturated vapour. The bubble is located in infinite mass of incompressible liquid; initially its internal contents are in mechanical equilibrium (pressure and surface tension). The liquid and bubble are initially at temperature T_∞. The initial non-condensable gas partial pressure is p_{GO}, while that of the vapour pressure is $p_{vo} = p_{vsat}(T_\infty)$.

At time zero the system pressure is increased instantaneously to p_∞ and the collapse ensues.

Additional assumptions made in developing the model for cavitation breakdown include the following:

1. The pressure outside the bubble $p_L(t)$ does not remain constant and keeps changing as the bubble moves, i.e., $p_L(t)$ is function of time (t).
2. The temperature at the bubble wall T_R decreases or increases as the bubble grows or shrinks, i.e., T_R is function of time.
3. The liquid temperature at the reference point T_∞ remains constant.
4. The change in the surface tension of the liquid as the bubble growth is neglected since the range of temperature of the present experiment is small.
5. The compressibility of both liquid and vapour is neglected, and
6. The contents of the bubble are assumed to be at uniform temperature at any given time.

The pressure of the gas within the bubble can be estimated by the use of Henry's Law which states that the partial pressure of the gas is proportional to the concentration of dissolved gas at equilibrium:

$$p_G = \beta.\gamma \quad (8)$$

where β is the Henry's constant and γ is the dissolved gas constant. The Henry's constant and the dissolved gas constants were found to be varied with temperature. These variations have been found from the information given by Omega Engineering Inc. (2004) as follows:

$$\beta = 2.936 \text{ x } 10^{-35} T_\infty^{14.343} \quad (9)$$

and

$$\gamma = 1.47 \text{ x } 10^{16} T_\infty^{-6.166} \quad (10)$$

Therefore, the variation of the pressure of the gas within the bubble with temperature is given as follows:

$$p_G = 4.31592 \text{ x } 10^{-19} T_\infty^{8.2774} \text{ N/m}^2 \quad (11)$$

The absolute viscosity (μ) was found to be varied with water temperature. These variations have been obtained from Handbook of Tables for Applied Engineering Science. The variations of water viscosity with temperature in the range of temperature in the present experiments were found follow approximately a power law. Therefore, the viscosity is given by the following expression:

$$\mu = 2.04248 \text{ x } 10^{10} T^{-5.4} \text{ Pa.s} \quad (12)$$

Since the Rayleigh solution governs the initial bubble growth and also the collapse, it is assumed that the actual bubble growth is simply proportional to the initial growth rate, and that the constant of proportionality does not vary materially with temperature.

For $R \gg R_0$, Rayleigh gives:

$$\dot{R}^2 = \frac{4}{3}\frac{S}{\rho_L R_0} \quad (13)$$

and at time (t) the bubble radius is given by:

$$R = R_0 + \int_0^t \dot{R}\, dt \quad (14)$$

Since $\dot{R}$ is independent of time, equation (14) can be written as:

$$R = R_0 + \dot{R}t \quad (15)$$

Since $R \gg R_0$ at the breakdown it follows that:

$$\dot{R}t \gg R_0 \quad (16)$$

Therefore:

$$R = \dot{R}t \tag{17}$$

or

$$R = \sqrt{\frac{4}{3}\frac{S}{\rho_L R_0}}.t \tag{18}$$

R_0 is the initial radius of the bubble nuclei, the nature of which is unknown.

It is assumed that the bubble nuclei are carried in the fluid stream and constant in number (i.e. are neither created nor destroyed), and that in a de-aerated liquid the effect of pressure on nuclei radius is negligible, that is R_0 is constant and independent of temperature.

At the occurrence of breakdown condition, the cavitation spreads across the inlet passageway of the pump; this means that under such conditions the mean length of the cavitating region is constant, and independent of temperature, and that the area to flow is constant. Therefore, the growth time (t) is given by:

$$t = k/\dot{Q} \tag{19}$$

where $\dot{Q}$ is the volumetric flow rate and k is constant of proportionality. The flow rate and k are constant at a particular temperature for a given pump and liquid.

Accordingly substitution equation (19) into (18) the radius of the bubbles is given as:

$$R = \frac{\dot{Q}}{k}\sqrt{\frac{4}{3}\frac{S}{\rho_L R_0}} \tag{20}$$

Equation (20) shows that the bubble radius at the breakdown condition is constant for a given volumetric flow rate.

Figure 1 is the sketch of the bubble with surrounding liquid, the temperature, pressures, and densities at the appropriate points are labeled with the same symbols used in the equations which follow.

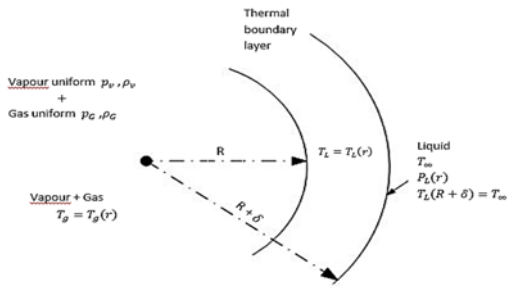

Fig. 1. Location of variables for thermodynamic effects study.

It was stated earlier that the heat for vaporization is drawn from the liquid. The volume of liquid which supplies this heat is given by:

$$V_L = 4\pi R^2 \delta \tag{21}$$

where δ is the thickness of the liquid in the thermal boundary layer giving up heat. Now, the heat energy drawn from the liquid is:

$$Q_L = 4\pi R^2 \delta \rho_L C_L \Delta T \tag{22}$$

The thermal energy required to fill the bubble with vapour in thermodynamic equilibrium with water is given by:

$$Q = \tfrac{4}{3}\pi R^3 \rho_V h_{fg} \tag{23}$$

Therefore, equating equation (22) and equation (23) for a heat balance over the bubble/liquid boundary, the local reduction in temperature (ΔT) is given by:

$$\Delta T = R h_{fg} \rho_V / (3 C_L \delta \rho_L) \tag{24}$$

In the earlier paper, Eisenberg (1961) gives a theoretical equation to estimate the liquid layer thickness of the diffusion length as:

$$\delta = \sqrt{\alpha t} \tag{25}$$

where α is the thermal diffusivity ($\alpha = k/\rho C_L$) and t is the vaporization time.

Substitution equation (15) into (14) the reduction in temperature at the bubble wall is given as:

$$\Delta T = (R h_{fg}/3 C_L \sqrt{\alpha t})\,(\rho_V/\rho_L) \tag{26}$$

The variation of C_L and α with temperature may be neglected in the temperature range between T(R) and T(∞) in the present experiments. R is the radius of the bubble and it is dependent on the volumetric flow rate Eq. (20).

The local reduction in temperature (ΔT) can be expressed in terms of the local pressure drop (Δp_V) as:

$$\Delta T = (dT/dp_V)\Delta p_V \tag{27}$$

The Clausius / Clapeyron equation can be used to approximate the slope of the vapour pressure/temperature curve:

$$\frac{dT}{dp_V} = T\big(1 - (\rho_V/\rho_L)\big)(\rho_L/\rho_V h_{fg}) \tag{28}$$

For conditions remote from the critical point, the approximation $\rho_L \gg \rho_V$ can be made and hence

$$dT/dp_V = \rho_L T/\rho_V h_{fg} \tag{29}$$

Therefore, the local reduction in pressure is given by:

$$\Delta p_V = \big(\rho_V h_{fg}/\rho_L T\big)\Delta T \tag{30}$$

Substituting equations (20) and (27) into (30), yields

$$\Delta p_V = 2\big(\rho_V h_{fg}/\rho_L\big)^2 \frac{\sqrt{\dot{Q}/k}}{3 C_L T_\infty}\sqrt{\frac{4S}{3\alpha\rho_L R_0}} \tag{31}$$

The solution of equations (4) and (31) together gives a complete understanding of the effect of the liquid temperature on the cavitation breakdown characteristics of pumps.

Unfortunately, this is difficult because of the completed nature of equations as well as the lack of the measurements to estimate the variation of the pressure coefficient within the pump. Clearly the accuracy of solving equations (4) and (31) can be assessed only by considering the complete

understanding of the three factors, inertial, thermal and diffusive controlling the motion of a bubble is required. In addition, the spherical configuration of the bubble surface is unstable during the later stages of collapse. So that analysis based on the assumption of spherical symmetry cannot be rigorously correct. Therefore, the prediction of real bubble growth and collapse is a very complex problem, even in a zone of a constant superheat. In pumps the problem is even more difficult because the growth will occur in an indefinable adverse pressure gradient. This is due to the rapid growth and a collapse time which does not allow adequate time for an accurate measurement of pressure to be performed since human and instrument response time are slow compared to the rate of change in the fluctuations. Hence, only time averaged pressure profiles can be measured and these could be significantly different from the instantaneous profile which is dependent on the growth and collapse process.

As the fluid enters the impeller it will be subjected to a sudden acceleration, with an accompanying sharp reduction in pressure, it is in this region that the highest superheating will occur. Rapid fluctuations in the pressure have been noted the largest fluctuations being observed during the most rapid development and at breakdown conditions the oscillations were much less apparent. Accordingly, the discussion of model results will be based on similarity considerations. It is first assumed that the breakdown condition means the cavity is indefinitely long (i.e. supercavity) as the cavity extend over impeller blades. Under the breakdown condition any attempt to increase the flow by reducing the delivery pressure only produces an elongation of the cavity while the volumetric flow will remain constant and the delivery head sharply drops, meanwhile, the pressure gauge at the inlet of the pump reads minimum value. This implies that the definite bubble size which causes the breakdown is reached at the same geometrical location in the pump and it takes the same interval of time for bubbles to reach this location, for all temperatures. Accordingly, for a given discharge and speed in a given pump, it is expected that a kinematic similarity in bubble growth is existed for all temperatures. Therefore, the left-hand side of equation (4) is the same for all temperatures for a given discharge and speed in a given pump and also both the bubble radius and thickness of the liquid in the thermal boundary layer are the same. Moreover at a given flow rate, C_p and U_∞ remain the same.

From the previous discussions and assumptions and combining the foregoing equations (5), (7), (10), (11), (12), (17), (19), (20), and (21), equation (4) becomes:

$$4.31592\ \mathrm{x10^{-19}T_\infty^{8.2774}} - 8.16992\ \mathrm{K/\dot{Q}}\ \ \mathrm{T^{-5.4}} - (\rho W_1^2/2)\left[\sigma_b + (0.1903/T_\infty)\ \left(h_{fg}\,\rho_v/\rho_l\right)^2\sqrt{\dot{Q}/k}\right] = A \qquad (32)$$

Where k and A are constants for a given flow rate and speed in a given pump.

4. EXPERIMENTAL RESULTS AND DISCUSSION

In order to determine the effect of water temperature on cavitation breakdown, an extensive series of experiments were conducted. The test results of the variation of the blade cavitation number (σ_b) and the head ratio (H/H_o) at constant pump rotational speed and flow rate were plotted versus temperature of water.

Typical curves of the variation of the blade cavitation number with the head ratio from non-cavitating to cavitation breakdown condition at fixed flow rate of $4.96\text{x}10^{-3}$ m^3/s and rotational speed of 2600 rpm and water temperatures were varied from 20 °C to 85 °C are shown in Fig**.** 2. It represents a line of curves found in all the present extensive experiments.

The general trends of the head ratio versus blade cavitation number curves are that the head ratio attained nearly a constant value from the maximum blade cavitation number down to the point at which developed cavitation occurs. As the blade cavitation number decreased beyond the point of the developed cavitation, the head steeply till the breakdown of cavitation occurs. The cavitation breakdown has been taken as the point where the head ratio drops by 100 percent i.e., the head ratio sharply drops. At this point the pump head ratio breaks away at relatively constant monomeric suction lift i.e., constant blade cavitation number. At this condition the pressure gauge at the inlet of the pump reads minimum value which is nearly a few times of the vapor pressure corresponding to the bulk temperature of water.

Figure 2 indicates clearly the effect of water temperature on the breakdown blade cavitation number. This figure shows that at low temperature the breakdown blade cavitation number increases with increasing the water temperature and then decreases with increasing the water temperature. These characteristics of the variation of the blade breakdown cavitation number with temperature can be attributed to the thermodynamic effect (i.e., local cooling of water surrounding the cavity).

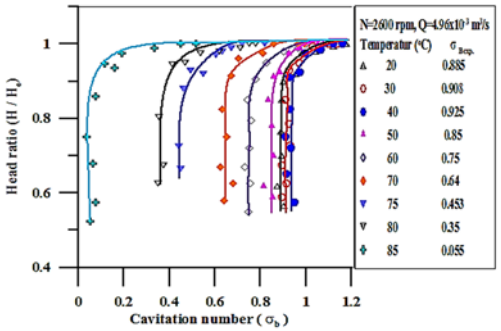

Fig. 2. Typical temperature effect on pump performance breakdown test series at constant speed (2600 rpm) and constant flow rate (4.96x 10^{-3} m^3/s).

This thermodynamic effect depends on the latent heat and the ratio of the saturated vapour density to

water density which is function of water temperature. Cold water gives small thermodynamic effect due to its low vapour pressure and low saturated vapour density, while hot water produces a significant thermodynamic effect due to its higher vapour pressure and high saturated vapour density. Therefore, the thermodynamic effect in terms of temperature difference ΔT or vapour pressure difference Δp_v is negligible at low temperatures but becomes very significant at high temperatures. As an example two different water bulk temperatures, 20 ^oC and 80 ^oC are considered. From the thermodynamic properties of water 20 ^oC and 80 ^oC, the thermodynamic effect parameter ($\rho_v h_{fg} / \rho_L$) in eqn (31) is multiplied by about 23 when passing from 20 ^oC and 90 ^oC.

Observation and photography of breakdown of cavitation patterns in the impeller of the tested centrifugal pumps were carried out under various water temperatures varied from 30 ^oC to 90 ^oC and constant rotational speed of 3000 rpm and flow rate ratio (Q/Q_{opt}) of 0.8 ($Q=5.43 \times 10^{-3}$ m^3/sec). The observation of cavitation breakdown was achieved by naked eye with the help of stroboscopic lighting through a transparent Perspex impeller casing. The photographs of cavitation breakdown were taken by a Song digital still camera. Photographs illustrating the breakdown cavitation patterns at various water temperatures are shown in Fig. 3.

In general, Fig. 3 illustrates that when breakdown condition is reached the cavity appears to be a fixed sheet attached to be the blade surface and being at the trailing edge of the blades and extends along the whole blades and its length appears to be independent of the water temperature. At low temperature of 30 ^oc, large milky cavity occurs along the suction surface of the blades. At the end of the cavity length, the cavity moves with vortex motion towards the pressure side of the blades. This may attributed to the non-uniformity of peripheral velocity components which causes transversal vortex through the whole space of the impeller channel.

With further increase in temperature (T=50 ^oC) the colour of the cavity remains the same and the cavity increases in its volume, i.e., becomes wider. Also, a limited length of cavity has been appeared on the pressure side of the blades. At higher temperatures (70 ^oC and 90 ^oC) the photographs show that the cavity is covered most of the impeller channel. In addition, at T=70 ^oC, the colour of the cavity becomes white with more brightness. However, at T=90 ^oC the coulor of the cavity becomes white with glassy contour appearance.

The change of the cavity colour between low and high temperature may attributed to the thermal effect. At low temperature the density of saturated vapour is low and the mass rate of evaporation of water needed is small. This means that the amount of which the temperature of the cavity interface falls below the bulk temperature of the water is also small (thermodynamic effect). Consequently, the vapour pressure in the cavity only falls slightly below the value of the vapour pressure at the bulk liquid temperature. Therefore, the difference between cavity pressure and pressure of the water far from the cavity is not influenced by thermal effects. At the high temperature the saturated vapour density can be many orders of magnitude lager than that at the low temperature, the mass rate of evaporation for the same cavity volume is much larger. Thus the heat which must be conducted to the cavity interface is much larger which means that a substantial thermal boundary layer builds up in the liquid at the interface which in turn causes the change in the colour of the cavity. This cause the temperature in the cavity to fall well below that of the bulk liquid and this, in turn, means that the vapour pressure within the cavity lower than otherwise might be expected and is influenced considerably by thermal effects (thermodynamic effects).

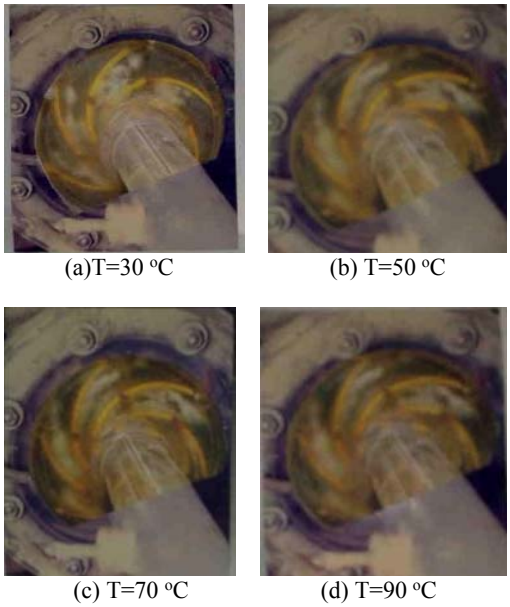

(a)T=30 ^oC (b) T=50 ^oC

(c) T=70 ^oC (d) T=90 ^oC

Fig. 3. Photographs of visulation cavitation breakdown condition in the impeller of centrifugal pump at various water temperature with constant flow rate ratio (Q/Q_{opt}) of 0.8 and rotational speed of 3000 rpm.

5. COMPARISON OF THEORETICAL MODEL WITH EXPERIMENTS

To compute the constants k and A in equation (29) it was necessary to use values of breakdown blade cavitation number from experimental results. Data from the present experimental results are used to obtain k and A for each rotational speed. Using these constants in equation (32) for predicting breakdown blade cavitation number at various temperatures can be obtained for the present pump.

The curves in Figs. 4-6 show the predicted values of the breakdown blade cavitation numbers at constant rotational speed and constant flow rates with water temperature varied from 20 and 90 ^oC. As shown in these figures the present experimental data are well predicated by the present theoretical model.

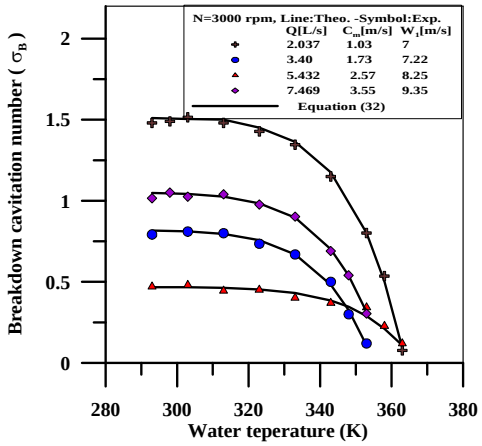

Fig. 4. Variation of theoretical and experimental breakdown cavitation number with water temperature at various pump volumetric flow rates and constant pump speed 3000 rpm.

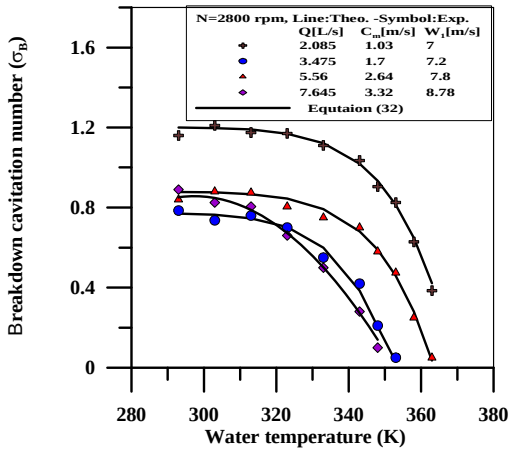

Fig. 5. Variation of theoretical and experimental breakdown cavitation number with water temperature at various pump volumetric flow rates and constant pump speed 2800 rpm.

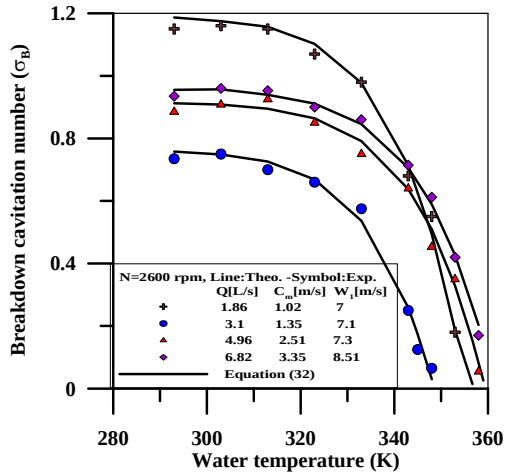

Fig. 6. Variation of theoretical and experimental breakdown cavitation number with water temperature at various pump volumetric flow rates and constant pump speed 2600 rpm.

Figure 7 shows a comparison between the predicted breakdown blade cavitation number and all experimental data at various pump operating conditions. This figure indicates that a good agreement between the theoretical and experimental breakdown blade cavitation numbers with correlation coefficient of 0.997. This agreement between the experimental and predicted values of breakdown blade cavitation numbers implies that the roles played by bubble dynamic, water temperature, rotational speed, and flow rate are consistent with the present analysis. However, the presented theoretical analysis in the present study is only a step towards better understanding the factors controlling the cavitation performance of the centrifugal pumps.

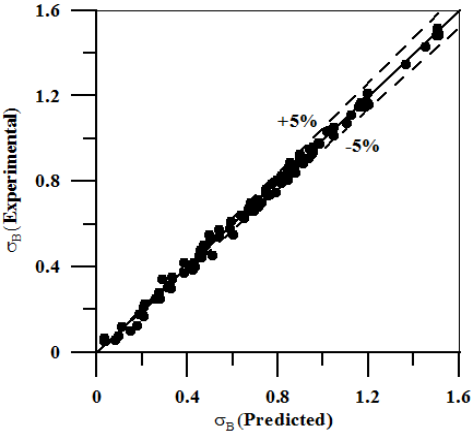

Fig. 7. Relation between theoretical and experimental breakdown cavitation numbers for all results.

Figure 8 to 13 show the present theoretical analysis applied to other investigators data. The agreement between the present theoretical analysis and the other investigator data is surprisingly good. This implies that the present assumptions about the breakdown condition in centrifugal pump were reasonable. In addition, the model gives good results when tested against different types of centrifugal pumps working at various operating conditions. Therefore, this theoretical result is very useful for the purpose of predicting the breakdown condition likely at various operating temperatures, flow rates and rotational speeds in a prototype from tests on a model with cold water since it is usually not possible to carry out cavitation tests under real higher temperatures. This is to help the centrifugal pump designer his pump to avoid the trouble of breakdown cavitation. The results obtained from the model reported here have raised some interesting points for further theoretical advances. However, some recommendations for future work regarding theoretical work can be made. It would be worthwhile and more useful to develop the present model to include some important thermo-physical parameters for liquids other than water to come nearer to practical cases. These parameters are compressibility, surface tension, viscosity and gradient of vapour pressure in respect to temperature (dp_v/dT). These properties exert a significant influence on the cavitation breakdown of pumps operating with hot liquid. Moreover, it would be more useful to develop the present model to

consider the dynamic equilibrium of clusters of cavitation bubbles instead of the dynamic equilibrium of a spherical bubble which was considered in the present model.

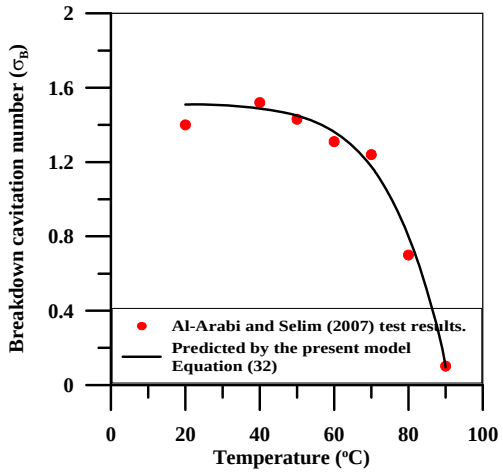

Fig. 8. Comparison between present model and test results (Al-Arabi and Selim, 2007).

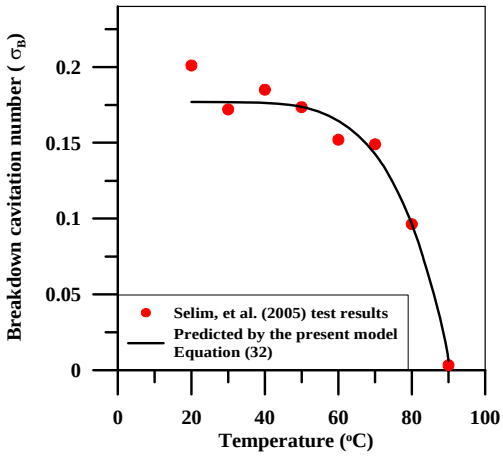

Fig. 9. Comparison between present model and test results (Selim *et al.*, 2005).

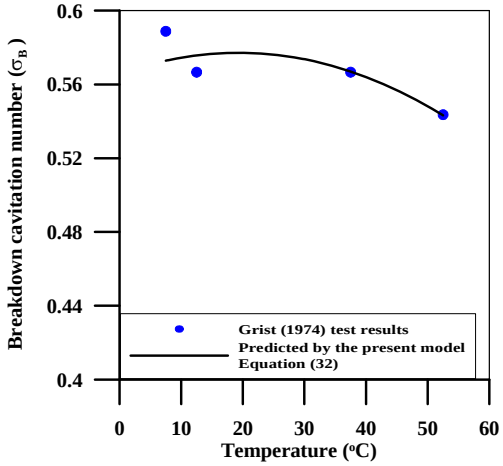

Fig. 10. Comparison between present models and test results (Grist, 1974).

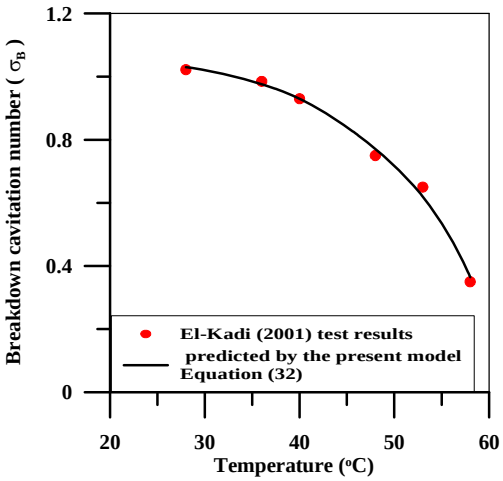

Fig. 11. Comparison between present model and test results (El-Kadi, 2001).

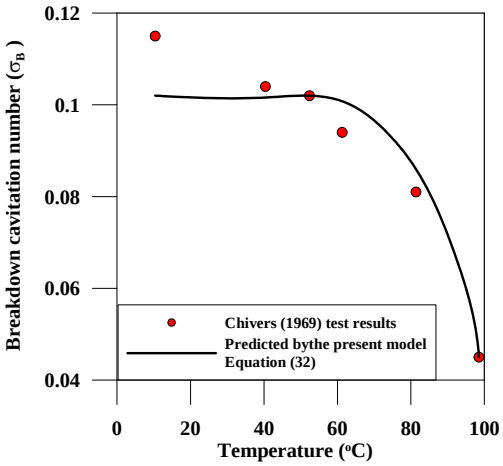

Fig. 12. Comparison between present model and test results (Chivers, 1969).

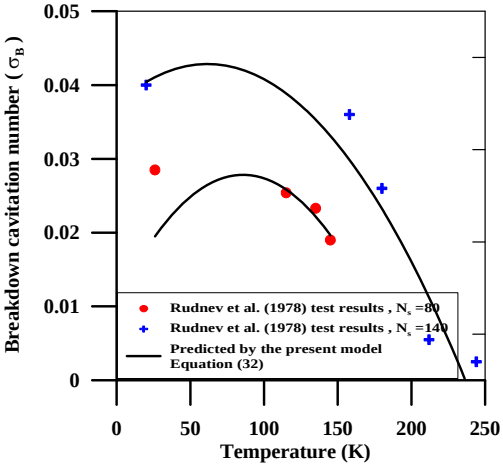

Fig. 13. Comparison between present model and test results (Rudnev *et al.*, 1978).

6. CONCLUSIONS

Extensive experiments were conducted to investigate the effect of various parameters on the breakdown cavitation number. The experiments were performed

at different temperatures various from 20 ºC to 90 ºC, rotational speeds of 2600, 2800 and 3000 rpm, and flow rate ranges from 1.86 to 7.645 liters/sec.

1. The extensive experimental results of the variation of head ratio versus blade cavitation number at various flow rates, water temperatures and rotational speeds showed that the head ratio obtained nearly a constant value from the maximum blade cavitation number down to point at which developed cavitation occurs, decreased beyond the point of developed cavitation and dropped sharply at the breakdown condition.
2. The experimental results of the effect of water temperature on the breakdown blade cavitation number indicated that at low water temperature the breakdown blade cavitation number increases with increasing the water temperature and then decreases with increasing the water temperature.
3. The predicted model of breakdown blade cavitation number presented herein includes many important parameters controlling the cavitation breakdown such as bubble dynamics, flow rate, rotational speed, water temperature, thermodynamic properties of water, and the gas pressure inside the cavity.
4. The predicted theoretical dependence of breakdown blade cavitation number on the water temperature, flow rate and rotational speed for the tested centrifugal pump agree well with the present extensive experiments. The agreements between experimental and theoretical breakdown blade cavitation numbers are surprisingly good.
5. The theoretical model has been shown to be valid for other investigators results. This implies that our assumptions for the present model were reasonable.
6. The present theoretical model is very useful for the purpose of assessing the breakdown blade cavitation number in centrifugal pumps at higher liquid temperatures from tests at low temperature. Therefore, it represents addition to knowledge in this aspect which could help the centrifugal pump user and designer to estimate the cavitation breakdown condition at various water temperatures and operating conditions.
7. It would be worthwhile and more useful to develop the present model to consider the viscosity, surface tension, compressibility and gradient of vapour pressure in respect to temperature of liquids other than water to come nearer to some practical cases.
8. In the cavitation breakdown model reported here, the dynamic equilibrium of a spherical bubble was considered, but in most practical cases several cavities interact. Therefore, it would be more useful for future work to consider the dynamic equilibrium of clusters of cavitation bubbles.

REFERENCES

Al-Arabi, A. B., and S. M. A. Selim (2007). A theoretical model to predict cavitation inception in centrifugal pumps. *5th Intr. Conference on Heat Transfer, Fluid Mechanics and Thermodynamics, Sun City, South Africa, AA2.*

Brennen, C. E. (1994). Hydrodynamics of pumps. *Oxford, England, Oxford University Press.*

Chivers, T. C. (1969). Temperature effects on cavitation in a centrifugal pump: theory and experiment. *Proceedings of the Institution of Mechanical Engineering 1 (2), 37-47.*

Eisenberg, P. (1961). Mechanics of cavitation, Section 12-I, Handbook of Fluid Dynamics, McGraw Hill Book Company, New York.

El-Kadi, M. (2001). Cavitation in centrifugal pump handling hot water. *Engineering Research Journal,Faculty of Engineering, Mataria, Cairo 77, 200-216.*

Gongwer, L. A. (1941). A theory of cavitating flow in centrifugal pump Impellers. *Trans. ASME, 63, 29-40.*

Grist, E. (1974). Net positive suction head requirements for avoidance of unacceptable cavitation erosion in centrifugal pumps. *Cavitation Fluid Machinery Group, Heriot – Watt University, Edinburg, Scotland, IMechE Conference Publication , London, England, Paper C 163-74.*

Hofmann, M., B. Stoffel, O. Coutier-Delgosha, R. Fortes-Patella and J. L. Reboud (2001). Experimental and numerical studies on a centrifugal pump with 2D-curved blades in cavitating condition. *CAV2001: session B7.005.*

Jain, P., H. Saini and A. Mathew (2016). Empirical study of cavitation performance in multi-stage centrifugal pump analyzing cavitation model. *International Journal of Advanced Technology in Engineering and Science 4(4), 26-31.*

Li, J., L. J. Liu and Z. P. Feng (2006). Two-dimensional analysis of cavitating flows in a centrifugal pump using a single-phase Reynolds averaged Navier Stokes solver and cavitation model. *Proceedings of the Institution of Mechanical Engineers, Part A: Journal of Power and Energy 220(7), 783-791.*

Li, W. G. (2014). Validating full cavitation model with an experimental centrifugal pump. *Task Quarterly 18(1), 81–100.*

Liu, H. L., D. X. Liu, Y. Wang, X. F. Wu and J. Wang (2013). Application of modified k-ω model to predicting cavitating flow in centrifugal pump. *Water Science and Engineering 6(3), 331-339.*

Mostafa, N., M. M. Karim and M. M. A. Sarkar (2016). Numerical prediction of unsteady behavior of cavitating flow on hydrofoils using bubble dynamics cavitation model. *Journal of*

Applied Fluid Mechanics 9(4), 1829-1837.

Omega Engineering Inc. (2004). The fundamental technical dissolved oxygen-conductivity and resistivity. *USA and Canada.*

Pearsall, I. S. (1972). Cavitation. *Mills and Boon Monograph ME/10.*

Pearsall, I. S. (1973). The supercavitating pump. Proceedings of the Institution of Mechanical Engineers *187(1), 649-665.*

Pierrat, D., L. Gros, G. Pintrand, B. Le Fur and P. h. Gyomlai (2008). Experimental and numerical investigations of leading edge cavitation in a helico-centrifugal pump. *The 12th International Symposium on Transport Phenomena and Dynamics of Rotating Machinery, Honolulu, Hawaii, February 17-22, ISROMAC12-2008-20074.*

Plesset, M. S. and A. Prosperetti (1977). Bubble dynamics and cavitation. *Ann. Rev. Fluid Mech. 9, 145-85.*

Rudnev, S. S., B. A. Kol'chugin and Kevorkov (1978). The effect of properties of the pumped fluid on cavitation in centrifugal pumps. *Fluid Mechanics –Soviet Research 7(3), 37-54.*

Selim , S. M., M. A. El-kadi , M. A. Younes, M. A. Hosien and I. R. Teaima (2009). The effect of solid-liquid mixture on cavitation characteristics of centrifugal pump. *Engineering Research Journal, Faculty of Engineering, Minoufiya University, Egypt 32(4), 511-520.*

Selim, S. M., M. A. El-kadi**,** M. M. M. El-Mayit and A. A. S. Al-Arabi (2005). Cavitation inception in centrifugal pumps at various operating conditions. *Engineering Research Journal, Faculty of Engineering, Minoufiya University, Egypt 28(3), 239-251.*

Tan, L., L. Zha, S. L. Cao, Y. C. Wang and S. B. Gui (2015). Cavitation performance and flow characteristic in a centrifugal pump with inlet guide vanes. *In IOP Conference Series: Materials Science and Engineering 72(3), 032028.*

Visser, F. C. (2005). Cavitation in centrifugal pumps and prediction thereof. *Presented at ASME Fluids Engineering Division Summer Conference, June 19-23, Houston, Texas, USA.*